https://doi.org/10.5194/egusphere-2025-3114
Preprint. Discussion started: 28 July 2025
© Author(s) 2025. CC BY 4.0 License.

General characteristics of the medium-scale gravity waves observed by airglow ground-based imaging over the Antarctic continent

Gabriel Augusto Giongo[1], Cristiano Max Wrasse[1], Pierre-Dominique Pautet[2], José Valentin Bageston[3], Prosper Kwamla Nyassor[1], Cosme Alexandre Oliveira Barros Figueiredo[4], Anderson Vestena Bilibio[1], Tracy Moffat-Griffin[5], Damian John Murphy[6], Toyese Tunde Ayorinde[1], Delano Gobbi[1], and Hisao Takahashi[1]

[1]Space Weather Division, National Institute for Space Research, São José dos Campos, SP, Brazil.
[2]Physics Department, Utah State University, Logan, UT, USA.
[3]Southern Space Coordination, National Institute for Space Research, Santa Maria, RS, Brazil.
[4]Federal University of Campina Grande, Campina Grande, PB, Brazil.
[5]Atmosphere, Ice and Climate Team, British Antarctic Survey, Cambridge, United Kingdom.
[6]Australian Antarctic Division, Kingston, Australia.

Correspondence: Gabriel Augusto Giongo (gabriel.giongo@inpe.br)

Abstract. Simultaneous airglow observations were conducted at various Antarctic stations to investigate the general characteristics of medium-scale gravity waves (50-800 km of horizontal wavelength) over the continent during 2022, the most recent year of simultaneous observations. Airglow data were collected from McMurdo (77.8° S, 166.6° E) and Davis (68.5° S, 77.9° E) on the eastern part of the continent, as well as from Rothera (67.5° S, 68.1° W) and the Brazilian Antarctic Station Commandant Ferraz (62.1° S, 58.4° W) on the Antarctic Peninsula. The keogram technique was used to analyze a portion of the wave spectrum that was not previously studied: waves with horizontal wavelengths larger than 100 km. A new analysis methodology, detailed in a companion paper, based on wavelet transform properties, was employed to extract wave parameters such as horizontal wavelength, period, and phase speed. Additionally, data from the WACCM-X model were utilized to calculate intrinsic and vertical parameters and momentum fluxes. Despite differences between the stations, the gravity wave parameters indicated larger wavelengths and phase speeds than those typically observed in tropical and mid-latitude regions. Anisotropy regarding wind filtering was inconclusive; waves propagated in all directions with varying speed ranges, and generally faster than the wind below the observation altitude. Vertical wavelengths ranged flatelly from 10 to 50 km, and momentum fluxes were generally below 20 m^2/s^2, resulting in a limited energy transport at the observation altitude (∼87 km) from these waves.

1 Introduction

The Earth's atmosphere has many horizontal motions of air masses that can lead the atmosphere to a temperature equilibrium different from the pure radiative equilibrium, allowing an adequate environment for life development. In addition to air motion, the atmosphere is rich in waves, which do not transport masses but energy and have an essential role in temperature equilibrium. One particular class of atmospheric waves is the so-called gravity waves, also known as buoyancy waves, which can propagate vertically and horizontally through the atmosphere. Gravity waves are an exciting topic in the atmosphere field due to their

https://doi.org/10.5194/egusphere-2025-3114
Preprint. Discussion started: 28 July 2025
© Author(s) 2025. CC BY 4.0 License.

vertical energy and momentum transport, which connects the atmospheric layers differently than the air masses (Holton, 2004; Fritts and Alexander, 2003). As these waves grow in amplitude while propagating vertically, their influence in the atmosphere increases in the upper atmospheric layers, making them the most important dynamic feature in the middle and upper atmosphere (Nappo, 2002).

Gravity wave observers have been interested in the Antarctic continent in recent years. Information on gravity wave propagation can improve global circulation models and forecast systems (Vosper et al., 2018; Geller et al., 2013). In addition, observations provide essential features of the dynamical basis of transient instabilities and irregular phenomena, which are difficult to foresee and hardly ever occur in models due to their simplifications (Kogure et al., 2018; Kalisch et al., 2014). Even after observations, explaining their occurrence remains challenging without estimating the associated conditions (Plougonven et al., 2013; Nielsen et al., 2009; Murphy et al., 2014).

Recent works have developed techniques for synthesizing the raw observations into the wave parameters and general wave characteristics (Hindley et al., 2019; Perrett et al., 2021; Figueiredo et al., 2018; Giongo et al., 2024). Models and secondary data sets help identify the occurrence of the waves with regard to general atmospheric behavior and understand their dynamic features (Xu et al., 2019; Wei et al., 2022). In that sense, wave occurrence and activity characteristics are related to the background atmospheric conditions, making the wave activity somewhat predictable (Plougonven et al., 2020; Becker and Vadas, 2020).

Observations within the Antarctic stratosphere were done using super-pressure balloons by Plougonven et al. (2013, 2017). Their results showed intense activity of gravity waves over the mountainous regions of the continent and islands over the ocean. The authors concluded that most of the wave activities in the stratosphere are orographic waves generated by terrain features. Waves generated by meteorological phenomena and low atmosphere systems are less frequent than in mid and low latitudes due to a less frequent occurrence of such phenomena in the polar regions (Nielsen et al., 2009; Matsuda et al., 2017; Kam et al., 2017). On the other hand, intense observations of gravity wave activity have been seen over the Antarctic continent at the mesospheric and ionospheric heights, leading to questioning what made such observations possible (Bageston et al., 2009; Hindley et al., 2019; Xu et al., 2024). Recently, studies raised the hypothesis of secondary gravity wave generations, which consist of a generation of waves from body forces generated by the turbulence of a primary wave breaking. Efforts to test such a hypothesis have been conducted by computational modeling and high-resolution observations (Wright et al., 2017; Vadas and Becker, 2019; Kogure et al., 2020).

According to the recombination hypothesis, waves seen above 70 km in height are secondary waves generated from the breaking of mountain waves or meteorological phenomena (Vadas et al., 2019). Mountain wave propagation to the mesosphere is constrained by the horizontal wind speed throughout the middle atmosphere and limited growth in wave amplitude. These conditions are not always observed (Pautet et al., 2021; Song et al., 2021). Another feature currently being discussed is the horizontal propagation of the waves. Several works have used it to examine the observational pattern of high atmosphere waves (Wright et al., 2017; Perrett et al., 2021). Observations would require extensive horizontal observations to confirm the hypothesis. However, simulations can show the possibility of horizontal propagation as a dependence on the wind's influence on the waves' movement (Sato et al., 2012; Fritts et al., 2019).

https://doi.org/10.5194/egusphere-2025-3114
Preprint. Discussion started: 28 July 2025
© Author(s) 2025. CC BY 4.0 License.

In this work, we analyze airglow medium-scale gravity waves observed at four stations along the Antarctic continent coast in 2022, using the recently developed methodology of Giongo et al. (2024). The main objective of the present paper is to characterize the medium-scale gravity waves over the Antarctic continent and study the typical behavior of the waves. Section 2 presents the instruments and methodology for wave observation, analysis, and parameter estimation. Section 3 summarizes the observations and the results related to the wave parameters and propagation directions. Section 4 discusses the results, while Section 5 concludes the work.

2 Instruments and Methods

Airglow imagers installed at the stations of McMurdo (77.8° S, 166.6° E, hereafter MCM), Davis (68.5° S, 77.9° E, hereafter DAV), Rothera (67.5° S, 68.1° W, hereafter ROT), and Commandant Ferraz's Brazilian Antarctic station at the Antarctic Peninsula (62° S, 58° W, hereafter CF) were the primary locations for this study. The imagers installed at McMurdo and Davis are the Utah State University (USU) all-sky cameras, while multifilter all-sky imagers were used at Commandant Ferraz and Rothera stations.

The USU all-sky imager comprises a Xenics infrared 320x256-pixel detector and a Fujinon fish-eye lens with a field-of-view of 180 degrees. It measures the broadband hydroxyl (OH) emission between ∼900 and ∼1700 nm. This bright emission originates from a ∼7 to 8 km-thick layer at ∼87 km altitude and is widely used as a tracer of the dynamical processes in the mesosphere and lower thermosphere (MLT) region. The data acquisition is controlled by a computer, which takes 3 s exposure time for each image every 10 s during nighttime (with the Sun ∼8 degrees below the horizon). It is important to note that the USU camera observes the OH layer in an infrared band (IR), while the multifilter cameras measure in the near-infrared spectrum (NIR), so they have different detection spectra, and the observed altitude layer is slightly different.

The instrument at CF and Rothera is a Keo Scientific Sentri camera; more information is available on their website (keoscientific.com/imagers). Images have a spatial resolution of 512x512 pixels and a temporal resolution of 2 min at CF and 4 min at ROT. The USU cameras operate automatically on winter nights and have operated simultaneously and almost uninterruptedly since 2012, providing a large amount of coincident data with the all-sky camera at CF. This study uses the airglow data from 2022, the most recent year of simultaneous observations from those four sites.

Images were preprocessed to linearize, project them to geographical coordinates, and correct the contrast, brightness, and noise. After the initial processing of the images, Keograms were prepared to identify the medium-scale gravity waves. The spectral analysis is based on the wavelet transform to obtain gravity wave parameters. The spectral analysis code can identify the waves in keograms using the wavelet transform to calculate the horizontal wavelength, period, phase speed, and phase propagation direction from the wavelet reconstruction properties. More details on the analysis and amplitude correction methodology can be obtained in the companion paper by Giongo et al. (2024).

As the images of the USU cameras are smaller, the vertical series composing the keograms were re-gridded to a 512-pixel grid to avoid changes in the analysis code and in the methodology widely discussed by Giongo et al. (2024). Temporal resampling to a resolution of 1 min was performed with no loss of quality in the analysis procedure. Amplitude correction

https://doi.org/10.5194/egusphere-2025-3114
Preprint. Discussion started: 28 July 2025
© Author(s) 2025. CC BY 4.0 License.

followed the described method, except for the time-difference image correction, which was not necessary for the observations done with the USU camera, which provided a very good response for the short-period gravity waves (20-120 min). Inaccuracies due to this different treatment were tested, and no considerable differences were observed in the results.

Wind and temperature data from the Whole Atmosphere Community Climate Model Extended (WACCM-X) were used to calculate the intrinsic phase speed, period, and squared vertical wavelength profile. These calculations assessed the propagation conditions near the observation altitude and estimated the propagating waves' vertical wavelength and momentum fluxes.

The intrinsic horizontal phase speed ($c_{int} = c - u_0$), and the vertical squared wave-number were calculated following Nappo (2002):

$$m^2 = \left[\frac{N^2}{(c-u_0)^2} + \frac{u_{0zz}}{(c-u_0)} - \frac{1}{H}\frac{u_{0z}}{(c-u_0)} - \frac{1}{4H^2} - k^2 \right]. \tag{1}$$

where u_0 is the horizontal wind in the wave phase propagation direction and u_{0z} and u_{0zz} the first and second derivative of the horizontal wind.

For this study, all the terms were considered in the calculation, including buoyancy and scale height. Both terms involving the wind, wind shear, and wind curvature were used after tests were performed to validate their use. The wind derivatives become essential for the scale of the waves, although they are generally disregarded in the study of small-scale gravity waves. Wind shear and curvature are complementary; having both in the calculation is essential. Vertical wavelengths of the observed waves were assigned to an altitude of 86 km, as well as the intrinsic periods and phase speeds. The intrinsic period is calculated as a function of the intrinsic phase speed by $\tau_{int} = \frac{\lambda_h}{c_{int}}$.

For the propagating waves, the amplitudes, with the corrections described in the methodology, were used to calculate the momentum fluxes following the work by Vargas et al. (2007) using the cancellation factor determined by simulations:

$$MF = -\frac{1}{2}\frac{g^2}{N^4}\frac{m}{k}\omega^2 \left(\frac{I'}{CF}\right)^2 \tag{2}$$

where the $CF = I'_{\%}/T'_{\%}$ is the cancellation factor estimated by modeling traveling waves throughout the observations' theoretical layers. It is generally an asymptotic function of the vertical wavelength. In this work, we used the coefficients of the CF fitting given by Vargas et al. (2021) for medium-scale gravity waves.

3 Results

Observations of the waves primarily occurred during clear night sky conditions, specifically when the moon was absent and no clouds or auroras obstructed the field of view. Figure 1 illustrates the number of identified waves each month for every station, with colors distinguishing the data for each location. The total count of observed waves was 46 at the CF station over 18 nights of good observation. The observed wave counts for the other stations—ROT, MCM, and DAV—were 82, 144, and 57, respectively, with corresponding valuable nights of 30, 42, and 23. Observations among the different observatories were rarely coincident. However, a notable increase in wave occurrences was observed as winter approached, and there was a lack

https://doi.org/10.5194/egusphere-2025-3114
Preprint. Discussion started: 28 July 2025
© Author(s) 2025. CC BY 4.0 License.

of observations during June at the Rothera station. In contrast, MCM recorded most observations during the winter months. Overall, the primary occurrence of wave observations was during July.

The observations are directly related to the number of useful available nights of observation and the duration of the observation windows, which are longer at McMurdo Station. This is expected because we know that gravity waves are consistently present in the observed regions; however, we need clear observations to identify and analyze them effectively.

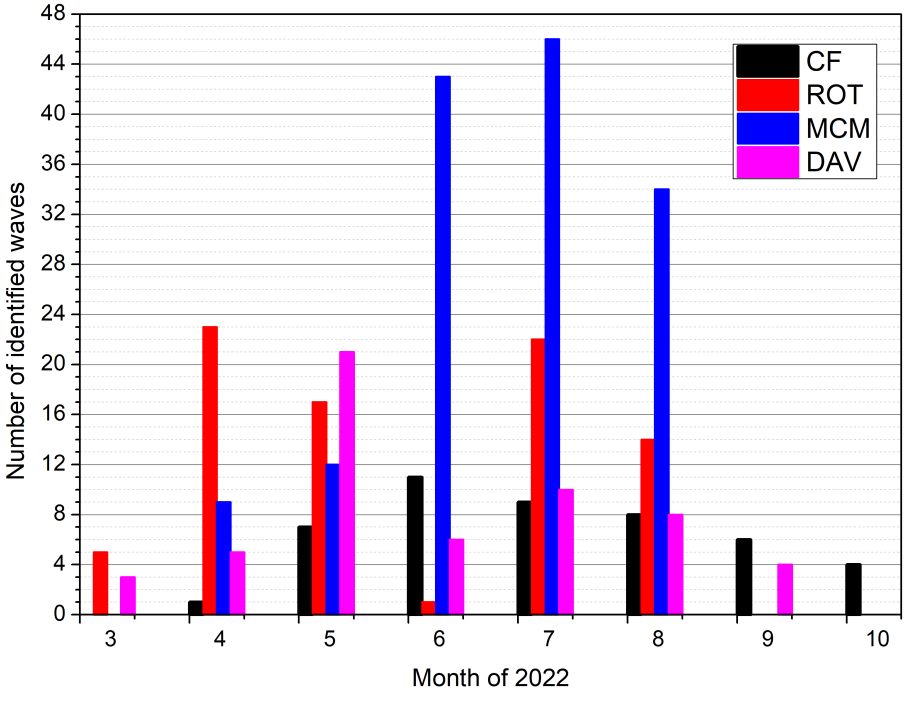

Figure 1. Histogram of the number of observed waves along the months of 2022 for each observation site. Histograms are sorted in colors for each observation site: Commandant Ferraz (CF) in black, Rothera (ROT) in red, McMurdo (MCM) in blue, and Davis (DAV) in magenta.

3.1 Gravity wave characteristics

Figure 2 presents the observed gravity wave parameters obtained from the spectral analysis, including horizontal wavelength, observed period, horizontal phase speed, and relative amplitude. The colors are sorted by observation site to differentiate the number of waves contributed by each observation site, although the parameters are separated in the following figure for better intercomparison.

The analysed MSGW on the Antarctic continent showed horizontal wavelengths from 50 to 1000 km, with concentration mainly between 100 and 400 km, and periods ranging from 20 to 180 min, with concentration between 30 and 60 min. Phase speeds ranged from 25 to 225 m/s, with primary concentration between 75 and 150 m/s, and relative amplitudes to a maximum of 7%, with concentration mainly between 1 and 3.5 %.

https://doi.org/10.5194/egusphere-2025-3114
Preprint. Discussion started: 28 July 2025
© Author(s) 2025. CC BY 4.0 License.

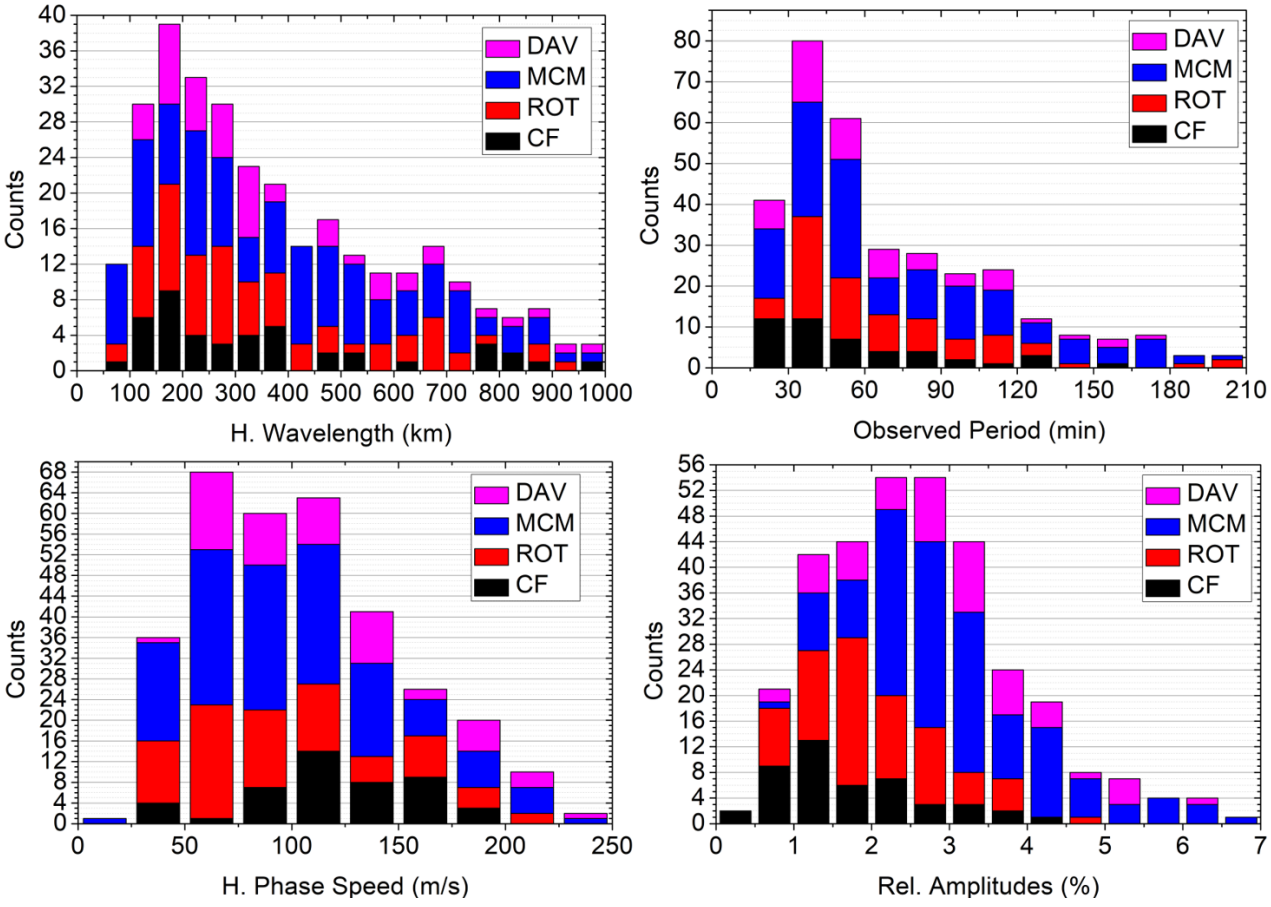

Figure 2. Histograms for the observed parameters: horizontal wavelength, observed period, phase speed, and relative amplitude for all observations accumulated.

Observed parameters for each of the observed sites are presented in Figure 3. The first row represents the parameters for the CF waves, the second row for the ROT waves, the third for the MCM waves, and the fourth for the Davis station. The first column displays the horizontal wavelengths for each station; the second column shows the periods; the third column indicates the phase speeds, and the fourth column presents the relative amplitudes. Colors are sorted by observation site.

Gravity waves observed in the CF region exhibited wavelengths ranging from 100 to 1000 km, with notable concentrations between 100 and 400 km and around 800 km. The observed periods were between 20 and 90 minutes, with some waves lasting over 120 minutes. The phase speeds of the waves were mainly distributed between 75 and 175 m/s; however, some waves exhibited phase speeds of less than 50 m/s, likely those associated with longer periods. The amplitudes varied primarily between 0.5% and 2.5%, indicating that the waves have a low influence on the airglow layer. Weather conditions largely constrained the observations.

https://doi.org/10.5194/egusphere-2025-3114
Preprint. Discussion started: 28 July 2025
© Author(s) 2025. CC BY 4.0 License.

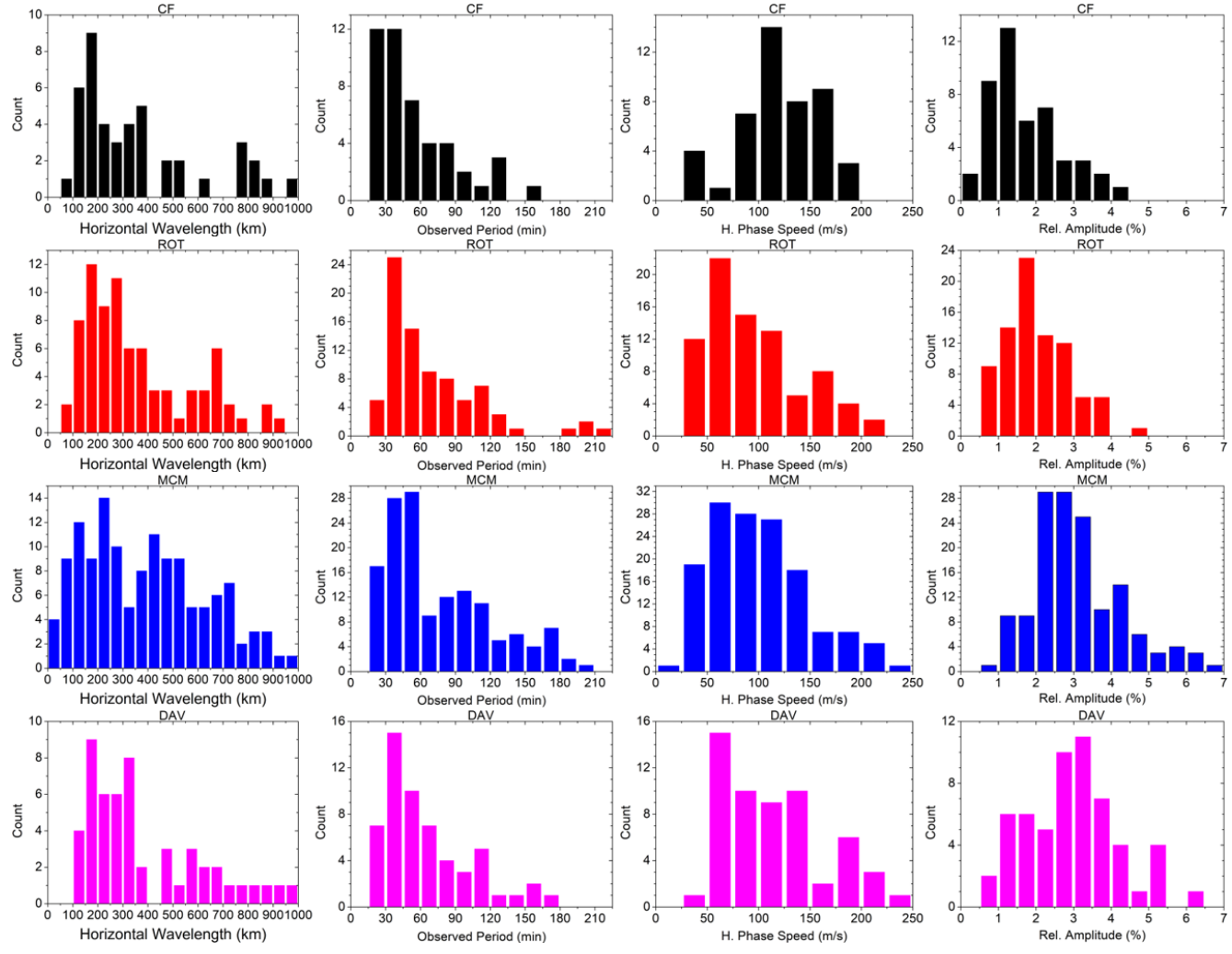

Figure 3. Histograms for the observed parameters: horizontal wavelength, observed period, phase speed, and relative amplitude for all Observation Sites. The first column is for the horizontal wavelength, the second is for the observed period, the third is for the observed horizontal phase speed, and the fourth is for the relative amplitude. The first, second, third, and fourth rows represent the CF, Rothera, McMurdo, and Davis wave parameters.

https://doi.org/10.5194/egusphere-2025-3114
Preprint. Discussion started: 28 July 2025
© Author(s) 2025. CC BY 4.0 License.

The main characteristics of the gravity waves observed in Rothera are similar to those from CF, although they show more concentration on the smaller wavelengths, between 100 and 300 km. The periods and phase speeds in Rothera are also shorter than those at CF, ranging mainly between 30 and 60 min, and 40 to 110 m/s for speeds. On the other hand, the amplitudes are notably higher, ranging between 1.0% and 3.0%. Interestingly, due to better weather conditions, Rothera had nearly twice as many wave observations as CF.

In contrast, the gravity waves observed at McMurdo Station exhibited longer wavelengths and were more widely distributed, with a peak from 100 to 600 km. The wave periods exhibited two peaks around 30-60 min and 90 minutes. The phase speed seems smaller than CF's but faster than the waves observed at Rothera, with the peak from 40 to 130 m/s. The amplitudes were significantly larger, with a peak between 2.0 % and 3.5 %. McMurdo Station has continuous observations during the winter nights (end of May to mid-July), resulting in a more extensive data set.

The analyzed gravity waves at Davis Station revealed shorter wavelengths, ranging mainly between 200 and 350 km, and periods concentrated below 60 min. Many faster waves were identified than for the other station, although the peak is between 50 and 150 m/s, below the peak of CF. Additionally, the main distribution of these waves resembled that found at CF Station. The amplitude distribution showed the most significant values spread among the four stations studied, with a peak of $3 \pm 1\%$. Some of the observations from Davis were excluded due to auroral contamination, as the station is located below the auroral oval.

3.2 Calculated wave parameters

This section presents the waves' intrinsic and vertical parameters calculated with the winds and temperature from the WACCM-X model at 86 km, typically the OH layer's central altitude at the polar regions. The vertical wavelength, intrinsic period, intrinsic phase speed, and momentum flux histograms are presented in Figure 4 for all observed waves. As the wind and temperature data used for these calculations are smooth and represent the real behavior of the atmosphere at the time of the wave observation in an averaged way, we should expect that mostly non-irregular values were identified for the calculated parameters. For better use, it is also recommended to observe wind and temperature data, like meteor radar-derived winds and lidar temperature, which are unavailable for all the observed sites.

The vertical wavelengths calculated for the observed MSGW presented values concentrated mainly between 10 and 50 km, with intrinsic periods more accentuated below 60 min, although the number of waves above 60 min is still considerable. Intrinsic phase speeds are more concentrated from 75 to 125 m/s. About momentum fluxes, they show a decreasing number of waves to a maximum of 50 m^2/s^2, while the main concentration is below 10 m^2/s^2, and a quasi-constant distribution between 15 and 50 m^2/s^2.

Histograms for the parameters as a function of the calculated parameters and observation site are shown in Figure 5. Histograms of the gravity waves for CF are shown in the first row (black), Rothera in the second row (red), McMurdo in the third row (blue), and Davis in the fourth row (magenta). Vertical wavelengths are shown in the first column, intrinsic period in the second column, intrinsic phase speed in the third column, and momentum fluxes in the fourth column.

https://doi.org/10.5194/egusphere-2025-3114
Preprint. Discussion started: 28 July 2025
© Author(s) 2025. CC BY 4.0 License.

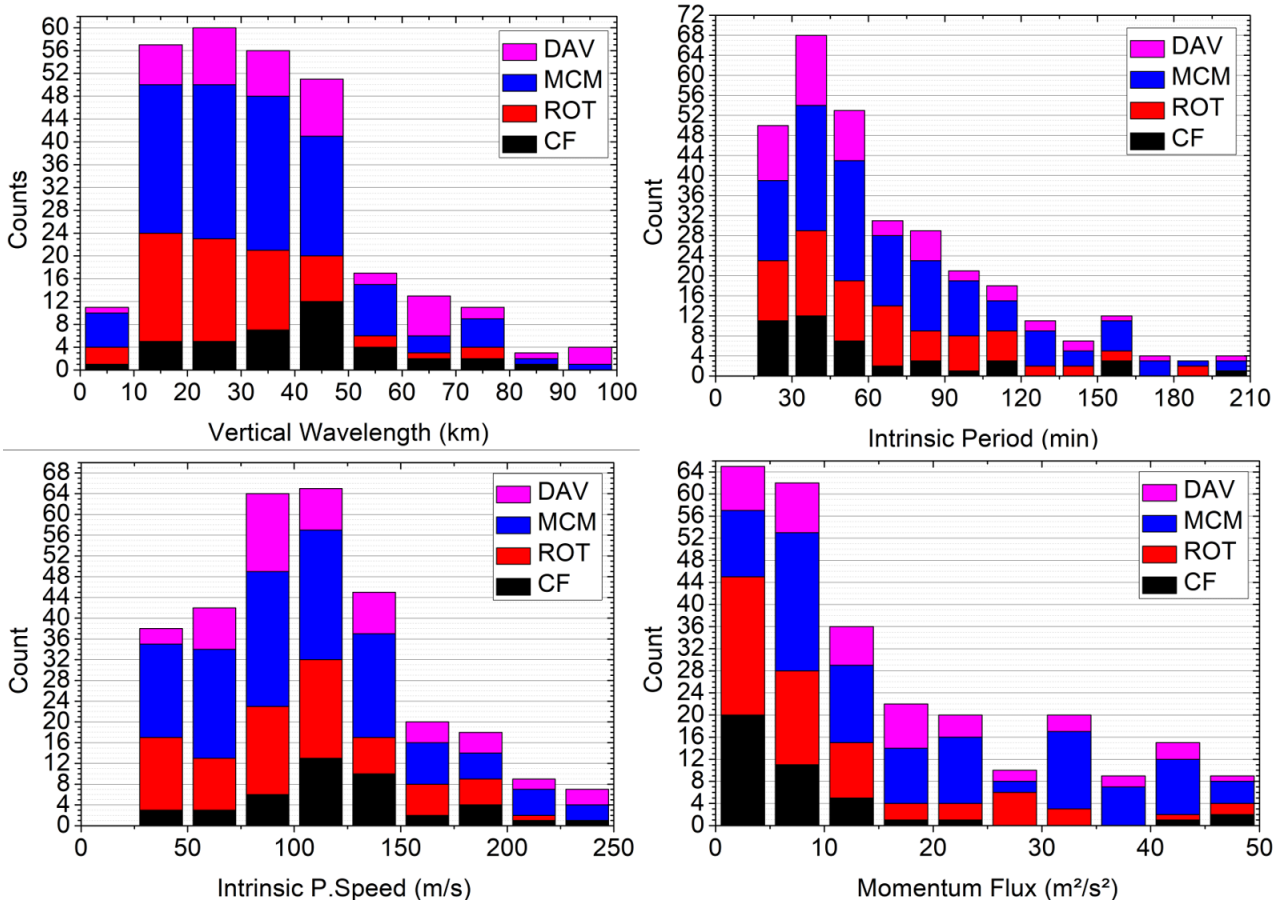

Figure 4. Histograms of the calculated parameters: vertical wavelength, intrinsic period, intrinsic phase speed, and momentum fluxes for all observation sites.

The analysis of gravity waves from CF revealed vertical wavelengths ranging from a few kilometers to 80 km, with the majority falling between 10 and 50 km. The intrinsic periods of the waves varied from 15 to 175 min, with a high concentration of values below 60 min. The intrinsic phase speeds ranged from 25 to 200 m/s, and in some cases, they reached up to 250 m/s. However, most waves exhibited intrinsic speeds between 75 and 150 m/s. Momentum fluxes reached a maximum of 50 m^2/s^2, while most values were below 15 m^2/s^2. It is important to note that the intrinsic parameters are similar to the observed ones due to the significant phase speed values relative to the wind speed delivered by the model.

Rothera waves showed lower vertical wavelength values, with a sharper concentration between 10 and 40 km. Although intrinsic periods and phase speed had a similar distribution to CFs, the values were more spread out, with a noticeable peak below 50 m/s in the wave phase speed. Momentum fluxes are similarly distributed, but more cases above 15 m^2/s^2 were obtained.

https://doi.org/10.5194/egusphere-2025-3114
Preprint. Discussion started: 28 July 2025
© Author(s) 2025. CC BY 4.0 License.

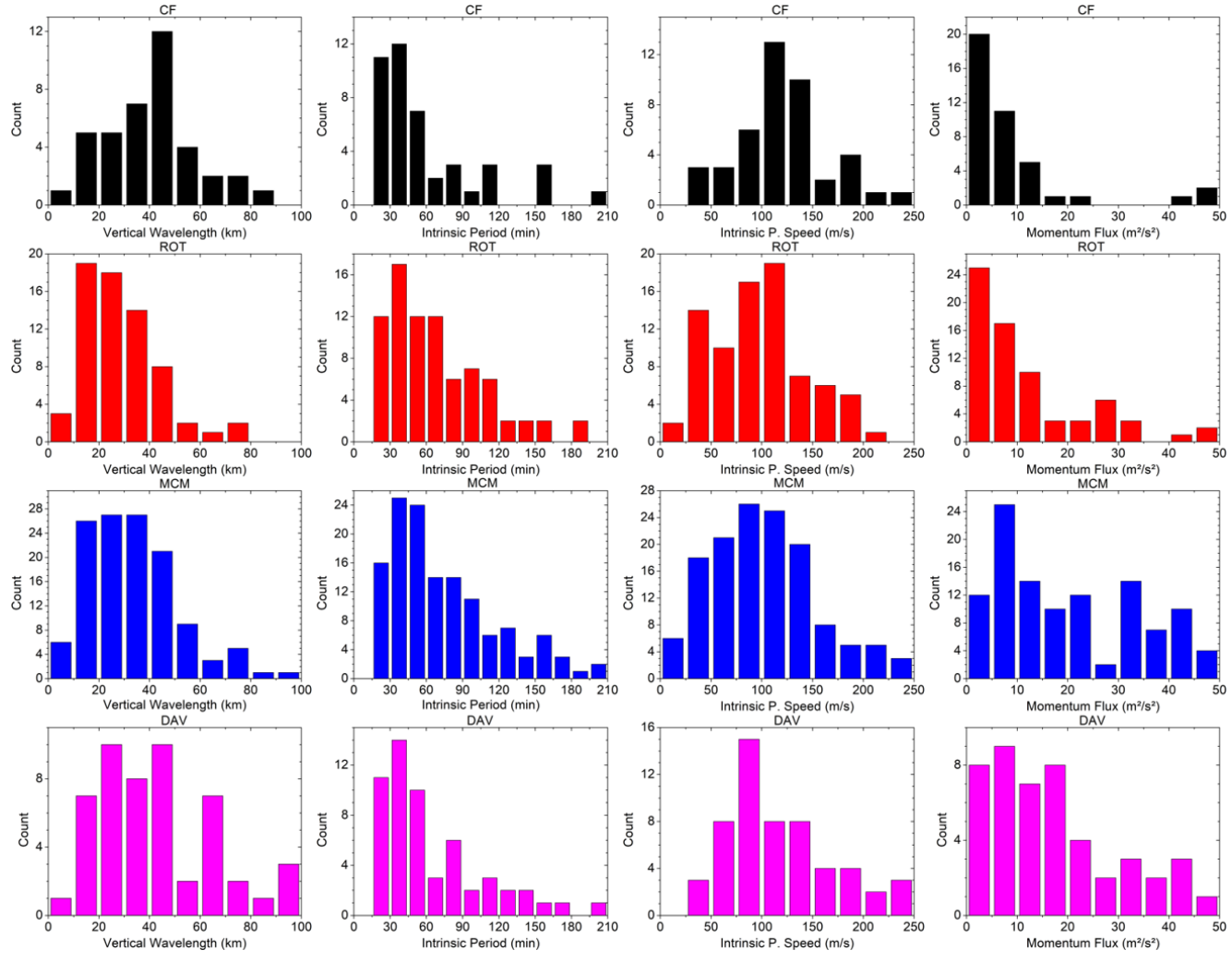

Figure 5. Histograms of the calculated parameters: vertical wavelength, intrinsic period, intrinsic phase speed, and momentum fluxes for all observation sites. The first column is for the vertical wavelength, the second is for the intrinsic period, the third is for the intrinsic horizontal phase speed, and the fourth is for the momentum fluxes. The first, second, third, and fourth rows represent the CF, Rothera, McMurdo, and Davis wave parameters.

https://doi.org/10.5194/egusphere-2025-3114
Preprint. Discussion started: 28 July 2025
© Author(s) 2025. CC BY 4.0 License.

Waves observed in McMurdo exhibited a nearly flat vertical wavelength distribution ranging from 15 to 50 km. The intrinsic periods displayed a distribution similar to that of CF waves. Intrinsic phase speeds were concentrated between 25 and 150 m/s, which is lower than that of CF waves. Momentum fluxes peaked between 5 and 10 m^2/s^2, while a uniform distribution was based on 45 m^2/s^2.

Davis showed a distribution of vertical wavelengths with a higher concentration of waves above 60 km. In contrast, the intrinsic periods were similar to those observed at other observation sites. The intrinsic speeds were primarily concentrated between 50 and 150 m/s. Momentum fluxes were uniformly distributed below 20 m^2/s^2. Additionally, a notable number of waves were recorded with momentum fluxes exceeding 20 m^2/s^2, which differed from the distribution seen at MCM. Furthermore, Davis identified a greater number of larger waves than those at CF and Rothera.

4 Wave propagation directions

Figure 6 shows the phase propagation direction of the gravity waves observed at each observation site. Figures 6a-d display angular histograms arranged in a wind-rose shape, illustrating the number of waves propagating within 30° sectors. Each histogram also shows the average horizontal phase speed of the waves within each interval. Figures 6e-h show the horizontal phase velocity vector of all waves for each site. This figure verifies the waves' preferential propagation conditions at each observation site and examines any potential anisotropy regarding phase speed, specifically the correlation between wave speed and direction.

Propagating and evanescent waves exhibit phase movements in the horizontal direction; however, evanescent waves lack momentum flux. Since the number of waves is relatively small, the authors chose not to segment this analysis into monthly or seasonal variations, as there is no statistical evidence to support such divisions.

Gravity waves observed at CF (Fig.6a,e) predominantly propagated to the east, with some waves propagating to the southeast, north, and southwest. Phase speeds were distributed regularly based on direction, with some waves traveling faster towards the southeast and others moving more slowly to the east and northeast. At Rothera, waves primarily propagated with a southward component, although there was a peak in the northeast direction. There was a slight preference for faster waves to move toward the northeast and southwest, while the average speeds were fairly uniform across other directions.

At McMurdo Station (Fig. 6c,g), the number of waves with an eastward component was clearly prominent, with faster waves favoring this direction. In contrast, slower waves predominantly propagated towards the south and west. At Davis Station (Fig. 6d,h), the direction of propagation also showed a preferred eastward component, along with a slight preference for the southward direction. Here, the faster waves were prone to propagate more towards the southwest and northeast. Overall, both stations exhibited both fast and slow waves in all directions.

Figure 7 shows the waves' momentum fluxes as a function of their phase propagation directions for each observation site. Gravity waves observed propagating to the north in CF are the waves with higher momentum fluxes, and those with smaller momentum fluxes propagate to the northeast and south (one exception). For Rothera, an anisotropy is seen, as the waves with higher momentum fluxes propagate with a southward component, while the waves propagating to the north have less MF, and

https://doi.org/10.5194/egusphere-2025-3114
Preprint. Discussion started: 28 July 2025
© Author(s) 2025. CC BY 4.0 License.

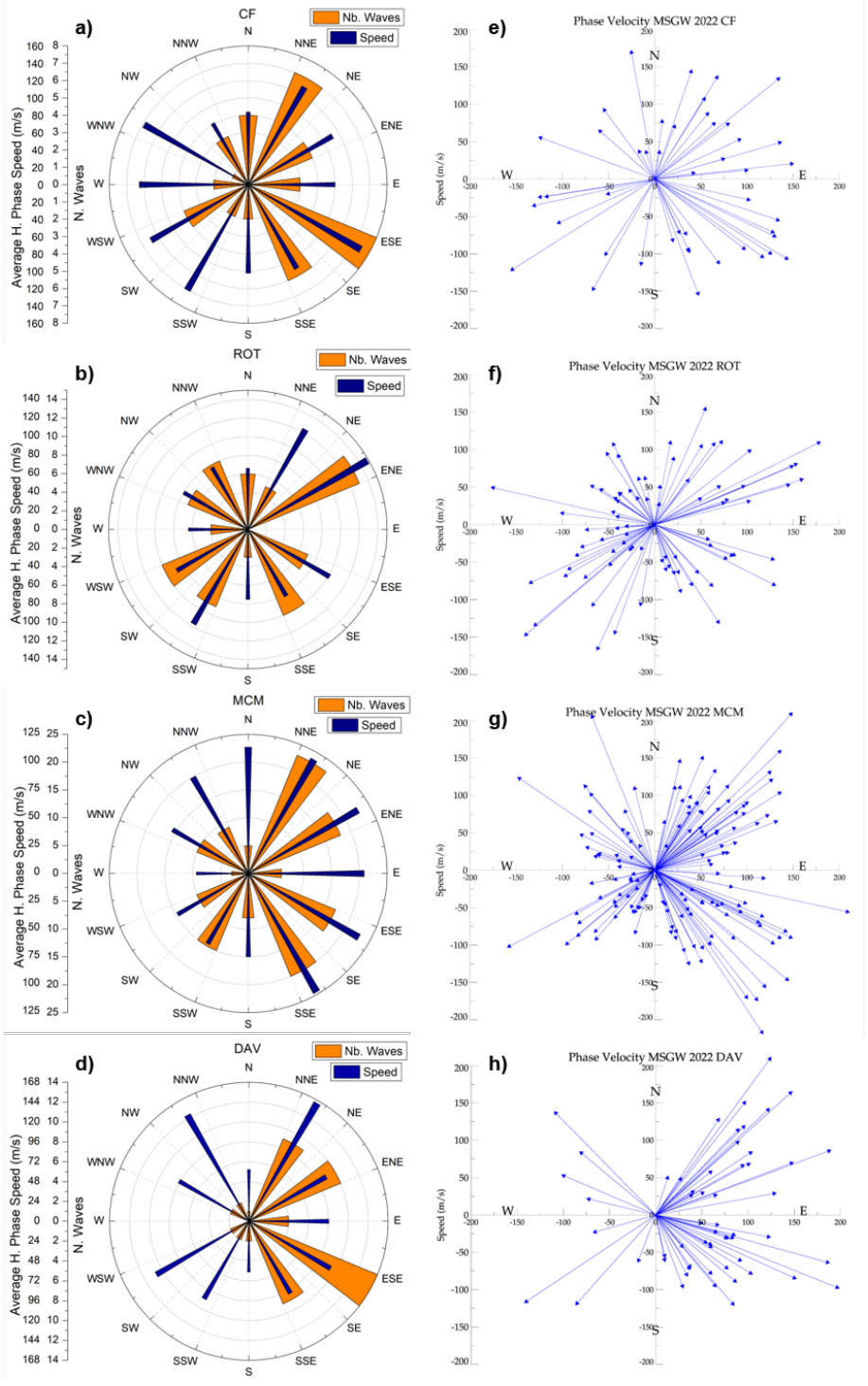

Figure 6. Phase propagation directions of the waves observed over all sites. a)-d) Histograms-windroses plot of the number of waves in each centralized angular sector, bins of 30°, in orange, and in blue, the average horizontal phase speed of the waves within that sector. e)-h) Phase velocity vectors for each observation site.

https://doi.org/10.5194/egusphere-2025-3114
Preprint. Discussion started: 28 July 2025
© Author(s) 2025. CC BY 4.0 License.

the MF below 5 m^2/s^2 are oriented in all directions. For MCM, few waves propagating to the southwest have momentum fluxes below 20 m^2/s^2, and in general, waves propagating to the south have more MF than those propagating to the north. At Davis, the waves with southward propagation have higher MF than the waves propagating northward. Notably, the anisotropy of the momentum fluxes seems to follow a meridional distribution, as the waves with more momentum propagate southward while those with less propagate to the north, with the opposite behavior for CF.

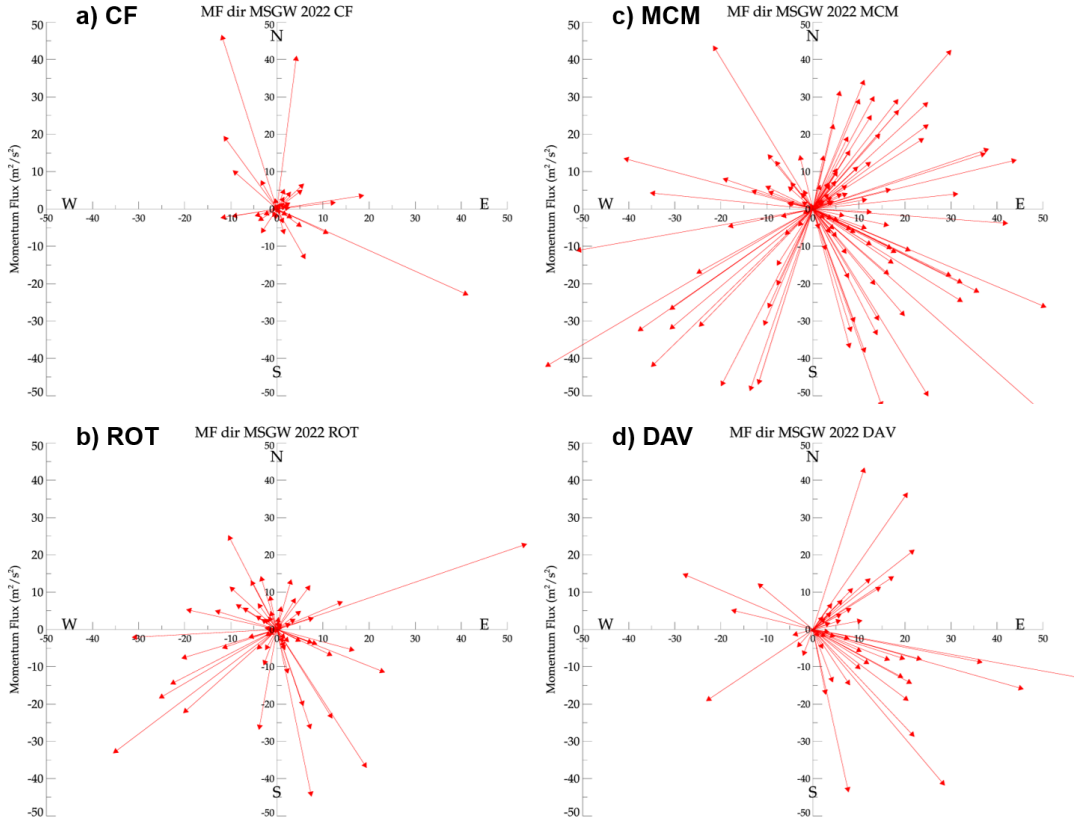

Figure 7. Momentum fluxes as a function of the horizontal propagation direction of the waves for each observation site. a) Waves observed at CF, b) ROT, c) MCM, and d) DAV.

Although the average wind roses do not indicate a correlation between faster waves and the east direction, faster waves are likely observed propagating toward the east or, at the very least, exhibiting a positive eastward component. This phenomenon is particularly evident at the CF and MCM observation sites. Furthermore, the eastward component is recognized as the preferred propagation direction for all stations, although this is less obvious for ROT. In contrast, the momentum fluxes show meridional anisotropy, with larger waves propagating southward and smaller waves moving north, except for CF, which displayed the opposite anisotropy while still remaining meridional. This behavior can be attributed to eastward-directed winds in the lower

https://doi.org/10.5194/egusphere-2025-3114
Preprint. Discussion started: 28 July 2025
© Author(s) 2025. CC BY 4.0 License.

layers, present at all observed sites during winter, such as the stratospheric polar vortex. Seasonal or monthly anisotropy was only weakly detected and are not presented here.

5 Discussions

The four observation sites studied are located in distinctly different areas regarding atmospheric motion. However, our analysis revealed similar behavior in the gravity wave parameters observed across the Antarctic continent through airglow imaging. Concerning the observed parameters, we noted that waves with wavelengths greater than 500 km, periods exceeding 2 hours, and speeds greater than 150 m/s are atypical compared to medium-scale internal gravity waves observed by airglow, as discussed later.

This report presents calculated parameters such as vertical wavelength and momentum flux for medium-scale gravity waves observed by airglow in a statistical manner for the first time. While some of these characteristics have been previously published for small-scale gravity waves through ground-based and satellite observations, as well as mountain waves exhibiting similar wavelengths, this is the first comprehensive statistical analysis of the medium-scale waves in the MLT. The propagation directions exhibited a weakly evident anisotropy, favoring eastward movement with likely faster waves in that direction. Numerous waves were detected traveling in various directions, and no significant seasonal variation was noted due to the limitations of the observations. Momentum fluxes displayed a meridional anisotropy, with larger waves moving southward while smaller ones headed northward, except for CF, which showed an inverse behavior. Further differences between the observed sites with respect to atmospheric conditions were not presented because, overall, no significant variations were noted.

The primary limitation of this work is the continuity of observations, which were disrupted by the moon and sun phases, meteorological events, and auroras, particularly at Davis Station. Consequently, seasonal variations could not be evaluated with statistical reliability. Nevertheless, future case studies can be undertaken for the most prominent or unique instances. While statistical reliability is evident in the presented wave parameters, it may only reflect general trends and differences between stations.

The annual characteristics of the sources of the observed waves could also not be related to the parameters of the waves. However, differences in the primary generation mechanisms of the waves observed at each station must exist and are linked to the geographical location of the observation sites. CF and ROT are situated on the Antarctic Peninsula, within the higher mountainous ridge, while CF is in a region influenced by a more vigorous polar vortex circulation. Therefore, these stations are expected to experience more intense wave activities, particularly those related to mountain and meteorological phenomena. MCM is positioned at the transition between the Transantarctic Mountains and the Ross Ice Shelf, but is found in an area with weaker stratospheric winds and is farther from the convective activities of lower latitudes. Consequently, the expected observations here will primarily involve mountain waves. Davis is located near an ice shelf region, yet is not close to any mountains; thus, the anticipated observations will arise from cyclonic activities occurring north of the station. Our study also refrained from examining the generation mechanisms of the waves separately and only considered their general characteristics. Future research is recommended to explore the generation mechanisms more thoroughly.

https://doi.org/10.5194/egusphere-2025-3114
Preprint. Discussion started: 28 July 2025
© Author(s) 2025. CC BY 4.0 License.

Previous studies did not provide information on the amplitudes and momentum fluxes of medium-scale gravity waves across different regions of the Antarctic continent. Recent research examining airglow-observed gravity wave (GW) parameters from various sites includes a study by Essien et al. (2018), which focused on medium-scale waves detected through the OH emission layer over São João do Cariri (7.4° S, 36.5° W) in Northeast Brazil, as well as a study by Taylor et al. (2009) conducted in the tropical central region of Brazil. The first study identified waves with horizontal wavelengths ranging from 50 to 250 km, periods ranging from 20 to 80 minutes, and phase speeds varying from 20 to 120 m/s. In contrast, the second study found waves with horizontal wavelengths of 50 to 200 km, observed periods from 20 to 60 minutes, and phase speeds ranging from 20 to 80 m/s, which are generally smaller and more concentrated than those reported in the first study. In Northeast Brazil, the waves predominantly propagated to the north and northeast, showing clear evidence of wind filtering influenced by stratospheric winds. Meanwhile, the waves primarily traveled southeastward and eastward in the central region. Additionally, the waves in low-latitude areas have similar periods, but their wavelengths and phase speeds are generally smaller and more concentrated.

In the northern polar region, the work of Suzuki et al. (2009) with observations at Resolute Bay, Canada (74°N), demonstrated medium-scale gravity waves on keograms of airglow, with horizontal wavelengths primarily ranging from 100 to 400 km, periods between 20 and 100 minutes, and phase speeds mainly from 60 to 100 m/s. The propagation directions were predominantly toward the west, with a significant number pointing north and south. Although their wave parameters were similar to those in our study, the propagation directions were entirely different from our observations. They also identified that the observed pattern resulted from wind filtering due to the stratospheric wind and connected the generation of the waves with near-ground phenomena of low pressure and ascending air in the troposphere east of the observation point.

A study conducted by Vargas et al. (2021) at a mid-latitude site using airglow observation employed a methodology that applied the Fourier transform directly to a sequence of images and extracted wave parameters without creating the keograms prior to the spectral analysis, thus not distinguishing between small and medium-scale waves. It resulted in gravity waves with periods of up to 50 minutes, similar to those observed in the current research. The differing methodology may explain why the horizontal wavelengths were sharply concentrated between 50 and 125 km, with phase speeds primarily below 80 m/s and vertical wavelengths ranging from 10 to 30 km. The recorded relative amplitudes were below 5%, while the momentum fluxes were under 20 m^2/s^2. Despite some differences in the parameters, our findings regarding amplitudes and momentum fluxes closely align with theirs.

Observations near the Antarctic Peninsula region have been conducted using satellites, such as the study by Wright et al. (2016) using limb and nadir satellite observations between 20 and 100 km height, which would observe waves with similar vertical wavelengths to this study. While they could not evaluate the periods, they found that the wavelengths displayed identical spectra to our research, and their amplitudes were greater. Their analysis suggested that the gravity waves might have been generated elsewhere or propagated horizontally from the source region, as they did not note a correlation between wave parameters and surface wind. A correlation of the wave energy with local wind suggested a Doppler shift of the observed waves into the observable spectra. Moreover, the research by Hindley et al. (2019) examined stratospheric gravity waves above the Antarctic continent and reported intense wave activity near the Antarctic coastal region, specifically around the 60° parallel. They found that the most intense and frequent waves occurred in mountain areas, such as the Antarctic Peninsula and the

https://doi.org/10.5194/egusphere-2025-3114
Preprint. Discussion started: 28 July 2025
© Author(s) 2025. CC BY 4.0 License.

transcontinental mountains. Although our study did not assess such spatial variations, we observed that the MCM and Davis observations exhibited more intense wave activity.

Furthermore, Zhao et al. (2015) investigated medium-scale gravity waves ($\lambda_h \approx$ 100-2000 km) traveling through the mesospheric polar clouds at an approximate altitude of 83 km during the polar summers. The analyzed waves have horizontal wavelengths ranging from 300 to 800 km. They also could not relate the observation to wind filtering, although they propose a direct connection between wave activities in the mesosphere and those in the lower atmosphere.

In the field of modeling, a recent study by Malhotra et al. (2025) used a high-resolution model of the atmosphere and ionosphere to analyze the global occurrence and propagation of gravity waves. They separated the wave activity by filtering the wind data in wavenumbers corresponding to 200 km and 600 km. They classified the primary global occurrences of medium-scale gravity waves into three distinct layers: the troposphere, stratosphere, and ionosphere. They found that a significant number of waves occurred in the troposphere, mainly near mountainous areas. At the same time, a widespread occurrence was noted in the stratosphere and ionosphere, potentially implying the MLT as well. The key finding indicated that this part of the spectra, especially above non-orographic regions, is likely secondary waves influenced by the vertical propagation conditions of the waves.

Matsuda et al. (2017) demonstrated the anisotropy of propagation directions related to the phase speed intensity of small-scale gravity waves at four stations around the Antarctic Continent: Halley (76° S, 27° W), Syowa (69° S, 40° E), McMurdo (78° S, 167° E), and Davis (69° S, 78° E). They found that the observed anisotropy indicated that the majority of these waves propagated westward and were classified as slow waves, while a smaller fraction propagated eastward with higher phase speeds. This behavior was attributed to stratospheric wind filtering. In contrast, the behavior of the medium-scale gravity waves we observed is not very similar to their findings, as the anisotropy driven by wind filtering is weak.

Kogure et al. (2023) observed waves in the OH that were even faster than the wind. The imbalance of the flow or secondary generation in the stratosphere could generate these waves. In contrast, waves that are slower than the wind could be generated in the troposphere, as they are oriented opposite to the wind. Therefore, the propagation direction related to the wind filtering anisotropy suggests possible source regions, although isolated cases still indicate the opposite.

The waves observed in our study have large phase speeds, many of which are faster than the polar vortex, enabling them to propagate from the troposphere despite the absence of a filtering pattern. Furthermore, simulation and observational studies (Malhotra et al., 2025; Kogure et al., 2023) suggest that above the stratospheric region, these waves are secondary waves generated by the breaking of tropospheric waves. In conclusion, we propose that the medium-scale gravity waves reported in this study may be both secondary waves and waves generated by tropospheric sources.

6 Conclusions

This study presents a novel analysis of medium-scale atmospheric gravity at four Antarctic stations, including two on the Antarctic Peninsula and two along the eastern coastal area. To investigate this part of the wave spectra, the keogram technique was utilized to analyze airglow images. The wave parameters were extracted using a wavelet transform and its properties, while

https://doi.org/10.5194/egusphere-2025-3114
Preprint. Discussion started: 28 July 2025
© Author(s) 2025. CC BY 4.0 License.

additional data were used to calculate the intrinsic and vertical parameters as well as the momentum fluxes of the medium-scale gravity waves.

The wave parameter results revealed a typical spectrum for these waves; however, larger wavelengths and phase speeds were observed compared to those in tropical regions. Vertical wavelengths varied widely, ranging from 10 to 80 km. Meanwhile, the momentum fluxes were generally low, typically under 20 m^2/s^2, suggesting that these waves do not possess sufficient energy to significantly influence the environment of the mesosphere and lower thermosphere (MLT). Both satellite observations and modeling confirm the presence of these waves over the Antarctic continent, but not all parameters can be thoroughly compared.

The directions of wave phase propagation did not show an apparent anisotropy concerning the wind filtering pattern. Notably, faster waves tended to propagate preferentially eastward, although waves of all types traveled in different directions and at varying speeds. In addition, momentum flux directions showed a meridional anisotropy, as the waves with more significant momentum fluxes propagated preferentially southward for ROT, MCM, and Davis, and northward for CF, representing a different direction from the waves generated by body forces (secondary waves). The average behaviors shown could not indicate whether the waves are primary waves. Determining whether a wave is primary or secondary remains challenging in the observational study of atmospheric gravity waves.

Data availability. Airglow images of the Comandante Ferraz Antarctic Station are available at the EMBRACE/INPE website.

Author contributions. Conceptualization, GAG, JVB, and CMW; Data curation, JVB, CMW, PKN, CAOBF, AB, TMG, DM, TA, and DG; Formal analysis, GAG and PDP; Methodology, GAG, CMW, CAOBF, and AB; Software, GAG, CMW, CAOBF; Validation, CMW, PDP, and HT; Visualization, GAG, CMW, PDP; Writing – original draft, GAG; Writing – review & editing, GAG.

Competing interests. The authors declare that they have no conflict of interest.

Acknowledgements. The authors express their gratitude to the Coordenação de Aperfeiçoamento de Pessoal de Nível Superior (CAPES), to the Conselho Nacional de Desenvolvimento Científico e Tecnológico (CNPq), to the Brazilian Ministry of Science, Technology, and Innovations (MCTI), and to the Brazilian Space Agency (AEB) for grant no. 20VB.0009. This work is part of the First Author's Ph.D. studies at the National Institute for Space Research (INPE), supported by CNPq (140401/2021-0) and Coordination for the Improvement of Higher Education Personnel (CAPES) finance code 001. The authors thank the CNPq/PROANTAR (307519/2022-8 and 440882/2023-0) and FAPESP (2019/05455-2 and 2023/06293-1) for supporting the revitalize/replacement of the instrumentation at Ferraz station. G. Giongo thanks the CAPES for the exchange scholarship and CNPq. PDP would like to acknowledge the National Science Foundation grant 1443730. Cosme Alexandre Oliveira Barros Figueiredo thanks the Conselho Nacional de Desenvolvimento Científico e Tecnológico (contract no.303871/2023-7) and Fundação de Apoio à Pesquisa do Estado da Paraíba (FAPESq) (contract no. 2417/2023) for supporting this research.

https://doi.org/10.5194/egusphere-2025-3114
Preprint. Discussion started: 28 July 2025
© Author(s) 2025. CC BY 4.0 License.

Cristiano M. Wrasse and Hisao Takahashi thank CNPq for the financial support (grants 310927/2020-0). Prosper K. Nyassor thanks the Fundação de Amparo à Pesquisa do Estado de São Paulo (FAPESP) for the financial support. The authors acknowledge the Brazilian Study and Monitoring of Space Weather (Embrace) Program at INPE for providing the all-sky airglow images used in this work and Utah State University for providing the images from McMurdo, Rothera, and Davis stations. Davis observations were supported through Australian Antarctic Science Projects 4445 and 4637. NERC NC PRESIENT (UK Polar Research Expertise for Science and Society) programme NE/Y006/78/1 provides support for the Rothera airglow imager.

https://doi.org/10.5194/egusphere-2025-3114
Preprint. Discussion started: 28 July 2025
© Author(s) 2025. CC BY 4.0 License.

References

Bageston, J. V., Wrasse, C. M., Gobbi, D., Takahashi, H., and Souza, P. B.: Observation of mesospheric gravity waves at Comandante Ferraz Antarctica Station (62° S), Annales Geophysicae, 27, 2593–2598, https://doi.org/10.5194/angeo-27-2593-2009, 2009.

Becker, E. and Vadas, S. L.: Explicit Global Simulation of Gravity Waves in the Thermosphere, Journal of Geophysical Research: Space Physics, 125, e2020JA028 034, https://doi.org/10.1029/2020JA028034, 2020.

Essien, P., Paulino, I., Wrasse, C. M., Campos, J. A. V., Paulino, A. R., Medeiros, A. F., Buriti, R. A., Takahashi, H., Agyei-Yeboah, E., and Lins, A. N.: Seasonal characteristics of small- and medium-scale gravity waves in the mesosphere and lower thermosphere over the Brazilian equatorial region, Annales Geophysicae, 36, 899–914, https://doi.org/10.5194/angeo-36-899-2018, 2018.

Figueiredo, C. A. O. B., Takahashi, H., Wrasse, C. M., Otsuka, Y., Shiokawa, K., and Barros, D.: Medium-Scale Traveling Ionospheric Disturbances Observed by Detrended Total Electron Content Maps Over Brazil, Journal of Geophysical Research: Space Physics, https://doi.org/10.1002/2017JA025021, 2018.

Fritts, D. C. and Alexander, M. J.: Gravity wave dynamics and effects in the middle atmosphere, Reviews of Geophysics, 41, https://doi.org/10.1029/2001RG000106, 2003.

Fritts, D. C., Wang, L., Taylor, M. J., Pautet, P.-D., Criddle, N. R., Kaifler, B., Eckermann, S. D., and Liley, B.: Large-Amplitude Mountain Waves in the Mesosphere Observed on 21 June 2014 During DEEPWAVE: 2. Nonlinear Dynamics, Wave Breaking, and Instabilities, Journal of Geophysical Research: Atmospheres, 124, 10 006–10 032, https://doi.org/10.1029/2019JD030899, 2019.

Geller, M. A., Alexander, M. J., Love, P. T., Bacmeister, J., Ern, M., Hertzog, A., Manzini, E., Preusse, P., Sato, K., Scaife, A. A., and Zhou, T.: A Comparison between Gravity Wave Momentum Fluxes in Observations and Climate Models, Journal of Climate, 26, 6383–6405, https://doi.org/10.1175/JCLI-D-12-00545.1, 2013.

Giongo, G. A., Wrasse, C. M., Pautet, P.-D., Bageston, J. V., Nyassor, P. K., Figueiredo, C. A. O. B., Bilibio, A. V., Gobbi, D., and Takahashi, H.: Medium-scale gravity waves observational methodology for antarctic airglow observations, EGUsphere, 2024, 1–20, https://doi.org/10.5194/egusphere-2024-3344, under revision, 2024.

Hindley, N. P., Wright, C. J., Smith, N. D., Hoffmann, L., Holt, L. A., Alexander, M. J., Moffat-Griffin, T., and Mitchell, N. J.: Gravity waves in the winter stratosphere over the Southern Ocean: high-resolution satellite observations and 3-D spectral analysis, Atmospheric Chemistry and Physics, 19, 15 377–15 414, https://doi.org/10.5194/acp-19-15377-2019, 2019.

Holton, J. R.: An introduction to Dynamic Meteorology, Academic Press, 2004.

Kalisch, S., Preusse, P., Ern, M., Eckermann, S. D., and Riese, M.: Differences in gravity wave drag between realistic oblique and assumed vertical propagation, Journal of Geophysical Research: Atmospheres, 119, 10,081–10,099, https://doi.org/10.1002/2014JD021779, 2014.

Kam, H., Jee, G., Kim, Y., Ham, Y.-b., and Song, I.-S.: Statistical analysis of mesospheric gravity waves over King Sejong Station, Antarctica (62.2°S, 58.8°W), Journal of Atmospheric and Solar-Terrestrial Physics, 155, 86–94, https://doi.org/10.1016/j.jastp.2017.02.006, 2017.

Kogure, M., Nakamura, T., Ejiri, M. K., Nishiyama, T., Tomikawa, Y., and Tsutsumi, M.: Effects of Horizontal Wind Structure on a Gravity Wave Event in the Middle Atmosphere Over Syowa (69 ° S, 40 ° E), the Antarctic, Geophysical Research Letters, 45, 5151–5157, https://doi.org/10.1029/2018GL078264, 2018.

Kogure, M., Yue, J., Nakamura, T., Hoffmann, L., Vadas, S. L., Tomikawa, Y., Ejiri, M. K., and Janches, D.: First Direct Observational Evidence for Secondary Gravity Waves Generated by Mountain Waves Over the Andes, Geophysical Research Letters, 47, https://doi.org/10.1029/2020GL088845, number: 17, 2020.

https://doi.org/10.5194/egusphere-2025-3114
Preprint. Discussion started: 28 July 2025
© Author(s) 2025. CC BY 4.0 License.

Kogure, M., Nakamura, T., Murphy, D. J., Taylor, M. J., Zhao, Y., Pautet, P., Tsutsumi, M., Tomikawa, Y., Ejiri, M. K., and Nishiyama, T.: Characteristics of Gravity Wave Horizontal Phase Velocity Spectra in the Mesosphere Over the Antarctic Stations, Syowa and Davis, JGR Atmospheres, 128, e2022JD037 751, https://doi.org/10.1029/2022JD037751, 2023.

Malhotra, G., Fuller-Rowell, T., Fang, T.-W., Yudin, V., Karol, S., Becker, E., and Kubaryk, A. M.: Medium-Scale Thermospheric Gravity Waves in the High-Resolution Whole Atmosphere Model: Seasonal, Local Time, and Longitudinal Variations, Journal of Geophysical Research: Atmospheres, 130, https://doi.org/10.1029/2024JD041810, 2025.

Matsuda, T. S., Nakamura, T., Ejiri, M. K., Tsutsumi, M., Tomikawa, Y., Taylor, M. J., Zhao, Y., Pautet, P., Murphy, D. J., and Moffat-Griffin, T.: Characteristics of mesospheric gravity waves over Antarctica observed by Antarctic Gravity Wave Instrument Network imagers using 3-D spectral analyses, Journal of Geophysical Research: Atmospheres, 122, 8969–8981, https://doi.org/10.1002/2016JD026217, 2017.

Murphy, D. J., Alexander, S. P., Klekociuk, A. R., Love, P. T., and Vincent, R. A.: Radiosonde observations of gravity waves in the lower stratosphere over Davis, Antarctica, Journal of Geophysical Research: Atmospheres, 119, 11,973–11,996, https://doi.org/10.1002/2014JD022448, _eprint: https://onlinelibrary.wiley.com/doi/pdf/10.1002/2014JD022448, 2014.

Nappo, C. J.: An Introduction to Atmospheric Gravity Waves, no. 85 in INTERNATIONAL GEOPHYSICS SERIES, Academic Press, ISBN 978-0-12-514082-9, 2002.

Nielsen, K., Taylor, M., Hibbins, R., and Jarvis, M.: Climatology of short-period mesospheric gravity waves over Halley, Antarctica (76°S, 27°W), Journal of Atmospheric and Solar-Terrestrial Physics, 71, 991–1000, https://doi.org/10.1016/j.jastp.2009.04.005, 2009.

Pautet, P., Taylor, M. J., Fritts, D. C., Janches, D., Kaifler, N., Dörnbrack, A., and Hormaechea, J. L.: Mesospheric Mountain Wave Activity in the Lee of the Southern Andes, Journal of Geophysical Research: Atmospheres, 126, https://doi.org/10.1029/2020JD033268, 2021.

Perrett, J. A., Wright, C. J., Hindley, N. P., Hoffmann, L., Mitchell, N. J., Preusse, P., Strube, C., and Eckermann, S. D.: Determining Gravity Wave Sources and Propagation in the Southern Hemisphere by Ray-Tracing AIRS Measurements, Geophysical Research Letters, 48, https://doi.org/10.1029/2020GL088621, 2021.

Plougonven, R., Hertzog, A., and Guez, L.: Gravity waves over Antarctica and the Southern Ocean: consistent momentum fluxes in mesoscale simulations and stratospheric balloon observations, Quarterly Journal of the Royal Meteorological Society, 139, 101–118, https://doi.org/10.1002/qj.1965, number: 670, 2013.

Plougonven, R., Jewtoukoff, V., Cámara, A. d. l., Lott, F., and Hertzog, A.: On the Relation between Gravity Waves and Wind Speed in the Lower Stratosphere over the Southern Ocean, Journal of the Atmospheric Sciences, 74, 1075–1093, https://doi.org/10.1175/JAS-D-16-0096.1, 2017.

Plougonven, R., de la Cámara, A., Hertzog, A., and Lott, F.: How does knowledge of atmospheric gravity waves guide their parameterizations?, Quarterly Journal of the Royal Meteorological Society, 146, 1529–1543, https://doi.org/https://doi.org/10.1002/qj.3732, 2020.

Sato, K., Tateno, S., Watanabe, S., and Kawatani, Y.: Gravity Wave Characteristics in the Southern Hemisphere Revealed by a High-Resolution Middle-Atmosphere General Circulation Model, Journal of the Atmospheric Sciences, 69, 1378–1396, https://doi.org/10.1175/JAS-D-11-0101.1, 2012.

Song, B., Song, I., Chun, H., Lee, C., Kam, H., Kim, Y. H., Kang, M., Hindley, N. P., and Mitchell, N. J.: Activities of Small-Scale Gravity Waves in the Upper Mesosphere Observed From Meteor Radar at King Sejong Station, Antarctica (62.22°S, 58.78°W) and Their Potential Sources, Journal of Geophysical Research: Atmospheres, 126, https://doi.org/10.1029/2021JD034528, number: 10, 2021.

Suzuki, S., Shiokawa, K., Hosokawa, K., Nakamura, K., and Hocking, W. K.: Statistical characteristics of polar cap mesospheric gravity waves observed by an all-sky airglow imager at Resolute Bay, Canada, J. Geophys. Res., 114, 2008JA013 652, https://doi.org/10.1029/2008JA013652, 2009.

https://doi.org/10.5194/egusphere-2025-3114
Preprint. Discussion started: 28 July 2025
© Author(s) 2025. CC BY 4.0 License.

Taylor, M. J., Pautet, P.-D., Medeiros, A. F., Buriti, R., Fechine, J., Fritts, D. C., Vadas, S. L., Takahashi, H., and São Sabbas, F. T.: Characteristics of mesospheric gravity waves near the magnetic equator, Brazil, during the SpreadFEx campaign, Annales Geophysicae, 27, 461–472, https://doi.org/10.5194/angeo-27-461-2009, 2009.

Vadas, S. L. and Becker, E.: Numerical Modeling of the Generation of Tertiary Gravity Waves in the Mesosphere and Thermosphere During Strong Mountain Wave Events Over the Southern Andes, J. Geophys. Res. Space Physics, 124, 7687–7718, https://doi.org/10.1029/2019JA026694, 2019.

Vadas, S. L., Xu, S., Yue, J., Bossert, K., Becker, E., and Baumgarten, G.: Characteristics of the Quiet-Time Hot Spot Gravity Waves Observed by GOCE Over the Southern Andes on 5 July 2010, Journal of Geophysical Research: Space Physics, 124, 7034–7061, https://doi.org/10.1029/2019JA026693, number: 8, 2019.

Vargas, F., Swenson, G., Liu, A., and Gobbi, D.: O(^{1}S), OH, and O_2 (b) airglow layer perturbations due to AGWs and their implied effects on the atmosphere, J. Geophys. Res., 112, 2006JD007 642, https://doi.org/10.1029/2006JD007642, 2007.

Vargas, F., Chau, J. L., Charuvil Asokan, H., and Gerding, M.: Mesospheric gravity wave activity estimated via airglow imagery, multistatic meteor radar, and SABER data taken during the SIMONe–2018 campaign, Atmospheric Chemistry and Physics, 21, 13 631–13 654, https://doi.org/10.5194/acp-21-13631-2021, 2021.

Vosper, S. B., Ross, A. N., Renfrew, I. A., Sheridan, P., Elvidge, A. D., and Grubisic, V.: Current Challenges in Orographic Flow Dynamics: Turbulent Exchange Due to Low-Level Gravity-Wave Processes, Atmosphere, 9, 361, https://doi.org/10.3390/atmos9090361, 2018.

Wei, J., Zhang, F., Richter, J. H., Alexander, M. J., and Sun, Y. Q.: Global Distributions of Tropospheric and Stratospheric Gravity Wave Momentum Fluxes Resolved by the 9-km ECMWF Experiments, Journal of the Atmospheric Sciences, 79, 2621–2644, https://doi.org/10.1175/JAS-D-21-0173.1, 2022.

Wright, C. J., Hindley, N. P., Moss, A. C., and Mitchell, N. J.: Multi-instrument gravity-wave measurements over Tierra del Fuego and the Drake Passage – Part 1: Potential energies and vertical wavelengths from AIRS, COSMIC, HIRDLS, MLS-Aura, SAAMER, SABER and radiosondes, Atmospheric Measurement Techniques, 9, 877–908, https://doi.org/10.5194/amt-9-877-2016, 2016.

Wright, C. J., Hindley, N. P., Hoffmann, L., Alexander, M. J., and Mitchell, N. J.: Exploring gravity wave characteristics in 3-D using a novel S-transform technique: AIRS/Aqua measurements over the Southern Andes and Drake Passage, Atmospheric Chemistry and Physics, 17, 8553–8575, https://doi.org/10.5194/acp-17-8553-2017, 2017.

Xu, S., Vadas, S. L., and Yue, J.: Quiet Time Thermospheric Gravity Waves Observed by GOCE and CHAMP, Journal of Geophysical Research: Space Physics, 129, e2023JA032 078, https://doi.org/10.1029/2023JA032078, 2024.

Xu, X., Xue, M., Teixeira, M. A. C., Tang, J., and Wang, Y.: Parameterization of Directional Absorption of Orographic Gravity Waves and Its Impact on the Atmospheric General Circulation Simulated by the Weather Research and Forecasting Model, Journal of the Atmospheric Sciences, 76, 3435–3453, https://doi.org/10.1175/JAS-D-18-0365.1, 2019.

Zhao, Y., Taylor, M., Randall, C., Lumpe, J., Siskind, D., Bailey, S., and Russell, J.: Investigating seasonal gravity wave activity in the summer polar mesosphere, Journal of Atmospheric and Solar-Terrestrial Physics, 127, 8–20, https://doi.org/10.1016/j.jastp.2015.03.008, 2015.